Indian Journal of Pure & Applied Physics
Vol. 62, January 2024, pp. 51-57
DOI: 10.56042/ijpap.v62i1.5169

Modeling the Parameters of p-i-n Solar Cells Based on $CH_3NH_3PbI_3$ Perovskite

Ferdinand Gasparyan

Yerevan State University, 1 Alex Manoogian St, 0025, Yerevan, Armenia
National Polytechnic University of Armenia, 105 Teryan St, 0046, Yerevan, Armenia

Received 26 August 2023; accepted 28 November 2023

The simulation of short-circuit current, open-circuit voltage, absorption coefficient, fill factor and efficiency of solar cell with p-i-n structure based on organo-trihalide perovskite semiconductors $CH_3NH_3PbI_3$ was carried out. Simulated data obtained for the short-circuit current density ~15÷31 mA/cm^2, the open-circuit voltage ~0.99÷1.03 V, the absorption coefficient ~10^4cm^{-1}, the fill factor ~82.1%÷84.8%, and the efficiency ~14.85÷ 27.2% are in good agreement with the results of previous numerical and experimental data for perovskites solar cells with similar composition and size. Closer to the edge of intrinsic absorption, both the short-circuit current and open-circuit voltage depend linearly on the wavelength of the incident irradiation. The calculations show the potential possibility of using perovskites in the design of tandem solar cells. The novelty of this work is the demonstration of the possibility of using thin layers of perovskite to convers solar energy. This material with direct bandgap energy provides good absorption of photons with energy>1.56 eV. In combination with the crystalline silicon, perovskite can broaden the absorption spectrum of irradiation, thereby increasing the power conversion efficiency of the tandem solar cells.

Keywords: Perovskite; Solar cell; Short circuit current

1 Introduction

Currently, solar cells (SC) based on organo-trihalide perovskite semiconductors ($CH_3NH_3PbI_3$, $CH_3NH_3PbI_{3-x}Cl_x$, and similar materials/ compositions) are attracting much attention due to their promising potential for applications. This is due to their unique properties: high absorption coefficient, adjustable energy band gap, long carrier diffusion lengths, good carrier transport properties, easy manufacturing, and low production costs[1-5]. Perovskites are successfully used in SCs based on planar p-i-n heterojunctions[6-11]. Optoelectronic applications of perovskites include high-efficiency tandem SCs[12-14], lasers[15,16], light-emitting diodes[17,18], optical sensors and photodetectors[7,19-21]. These materials can be used both as light collecting medium and as charge carrier transporter. Recently, record values of energy conversion efficiency (PCE) of 33.7% were observed for perovskite/Si tandem SCs[22], for perovskite SC fabricated at low temperatures the efficiency is about 31.2%[13], 29.15%[23]. PCE of over 25% is already common and is reported many times[24,25]. For perovskite/silicon tandem featuring black-Si with a tunnel oxide-passivated contact subcell, an efficiency of 28.2% has been observed[26]. Along with experimental studies, a lot of theoretical calculations and simulations are also carried out[27-29]. For conventional planar perovskite SC, coupled opto-electrical simulation was used[30]. Analytical and numerical simulations of perovskite SC were carried out to determine the requirements for the absorbing and contact layers to ensure efficient capture[5,31]. Using YT-KMPF as HTM achieved high PCE of 21.40% with V_{oc} of 1.08 V, J_{sc} of 25.76 mA cm^{-2}, and FF of 77% and in the case of carbazole-based HTM received $J_{sc} = 23.6$A/cm^2, $V_{oc} = 1.03$ V, FF=73%, PCE=17.5%.[32,33] For perovskite SCs with various designs and made with different technologies, very high FF values are reported: nanostructured SCs on textured silicon substrate 82.42%[28], for a p-i-n planar device 83%[34], using polymer-coated solvent annealing 85%[35], with nitrogen-doped TiO_2 electron transport layers 85.3%[36], with NiO_x hole transport layer more than 86%[37], using YT-KMPF as hole transport layer 77 %,[32] using carbazole-based hole transport layer 73%.[33] For short circuit current and open circuit voltage are received following values: 21.9 mA/cm^2 and 0.86 V[38]; 22.3 mA/cm^2 and 0.99 V[39]; 21 A/cm^2

*Corresponding author: (E-mail: fgaspar@myyahoo.com)

and 1.08 V[10]; 17.51 mA/cm^2 and 0.96 V;[28,40] 22.83 mA/cm^2 and 1.112 V[29]; 21.7-22.97 mA/cm^2 and 0.994-1.052[41] *etc*."

The $CH3NH_3PbCl_3$ perovskite has been investigated as a transparent conductor using the experimental method and density functional theory. The optical properties such as dielectric functions, refractive index and absorption coefficients of bulk $CH_3NH_3PbCl_3$ perovskite have been calculated[5].

The short-circuit current density and the PCE were 21.9 mA/cm^2 and 11.99%, respectively, for the sample with 210-nm-thick perovskite active layer[38]. Organic thin-film perovskite SCs are hundreds of nm thick and mainly consist of p–i–n junction[42].

The optical properties of the crystalline silicon–black silicon–perovskite tandem structure have been intensively studied theoretically and experimentally by our group in recent years[43-45]. Black silicon, when used in conjunction with crystalline silicon, makes it possible to increase the absorption of light at visible and near-IR wavelengths. The transport properties of charge carriers in perovskite absorbing materials are generally critical to the operation of photovoltaic devices using these materials. Theoretical studies of the electrical and optoelectronic properties of $CH_3NH_3PbI_3$ continue to be intensively discussed. In this paper, theoretical simulation in the drift approximation of the current transfer process in the p-i-n structure on the base of $CH_3NH_3PbI_3$ was carried out to optimize the electrical and geometric parameters for using in solar energy conversion. We investigate the performance of the p-i-n part of a solar cell with p-NiO/i-PVK/n-TiO_2/p-bSi/p-cSi/n-cSi complex structure to improve light absorption and hence its photovoltaic performance (here PVK is perovskite, bSi - black silicon, cSi - crystalline silicon).

2 Theory

Let's study the $p^+ - i(\nu) - n^+$ structure under irradiation, where the base $i(\nu)$ region is a direct band gap semiconductor $CH_3NH_3PbI_3$ with almost intrinsic conductivity. Base region is a thin-film absorbing semiconductor layer sandwiched between two charge-selective p^+ and n^+ lateral contacts. Fig. 1 shows the structure under study and its energy band gap behavior.

In most SCs, the series resistance is small ($< 0.1\ \Omega$) and the shunt resistance is large ($> 10^4\Omega$). They have relatively too small affect the I-V characteristics compared to other terms. Neglecting these small

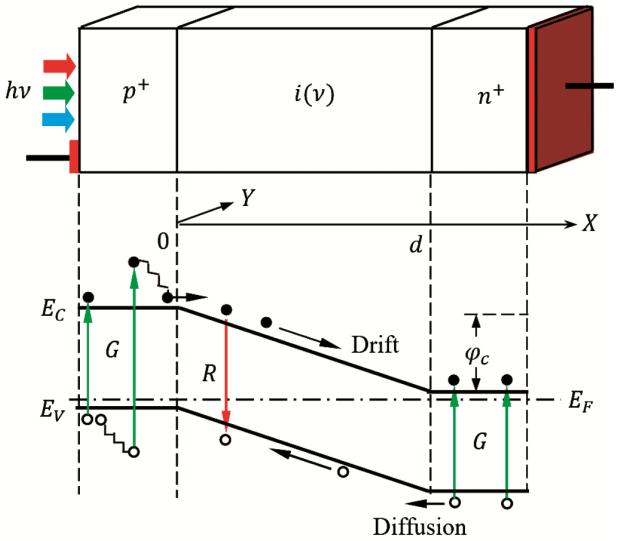

Fig. 1 — Schematic of the p-i-n structure under irradiation and its energetic band diagram. Here d is the thickness of i-base region, G and R (green and red arrows) are the generation and recombination rates of electron-hole pairs, φ_c is the contact potential, E_C, E_V are energies of conduction and valence bands, E_F is the Fermi equilibrium energy, correspondingly.

terms, the diode equation of a SC, under illumination, is simplified as below[46]:

$$J(\lambda) = J_d - J_{ph}(\lambda), J_d = J_s\left[exp\left(\frac{eV}{mkT}\right) - 1\right]. \quad ...(1)$$

Here J, J_{ph}, J_d and J_s are the diode total, photo-generated, dark and saturation current density, accordingly, V is the voltage, m is the diode ideality factor. At the Shockley–Read–Hall recombination $m = 2$. At zero voltage, short-circuit current J_{sc} flows. Open-circuit voltage V_{oc} can be calculatedin case the current equals to zero:

$$V_{oc} = \frac{mkT}{e} ln\left(\frac{J_{ph}}{J_s} + 1\right). \quad ...(2)$$

Under the influence of irradiation from the intrinsic absorption region, bipolar generation of photo carriers takes place in semiconductors. The non quilibrium concentration of electrons (n) and holes (p)will be

$$n = \Delta n + n_T \approx \Delta n, p = \Delta p + n_T \approx \Delta p. \quad ... (3)$$

For bipolar generation $\Delta n = \Delta p$. In Eqs. (2) and (3) e is the elementary charge, $\Delta n(\Delta p)$ and $n_T(p_T)$ are concentrations of non quilibrium excess photo carriers and thermal equilibrium electrons (holes), accordingly. Further we assume that $\Delta n \gg n_T, \Delta p \gg n_T$, and consequently $n \approx \Delta n, p \approx \Delta p$.

Next, we consider one-dimensional problem in the direction of current flow. Generated photo carries will create current with density J_{ph}, which will be sum of the electron (J_n) and hole (j_p) current densities:

$$J_{ph} = J_n + j_p = en\mu_n E + eD_n\frac{\partial n}{\partial x} + ep\mu_p E - eD_p\frac{\partial p}{\partial x}. \quad ...(4)$$

Here $\mu_n(\mu_p)$ and $D_n(D_p)$ are mobility and diffusion constants of electrons (holes). For further calculations we also use continuity equations:

$$\frac{1}{e}\frac{\partial J_n}{\partial x} = R_n - G(x), -\frac{1}{e}\frac{\partial J_p}{\partial x} = R_p - G(x). \quad ...(5)$$

Here G and $R_{n(p)}$ are the generation and recombination rates of electron-hole pairs in the ν – type base region, correspondingly:

$$R_n = \frac{n-n_T}{\tau_n} = \frac{\Delta n}{\tau_n}, \qquad R_p = \frac{p-p_T}{\tau_p} = \frac{\Delta p}{\tau_p}, G(x) = \eta(\lambda)\alpha(\lambda)F_0 exp(-\alpha x), \quad ...(6)$$

where τ_n and τ_p are the lifetimes of electrons and holes, correspondingly, $\eta(\lambda)$ is the internal quantum efficiency, $\alpha(\lambda)$ is the absorption coefficient, F_0 is the incident irradiation fluxand λ is the irradiation wavelength.

2.1 Drift Approximation Solution

When using the considered structure in SCs, the thickness of the $CH_3NH_3PbI_3$ layer should usually be on the order of hundreds of nm [$d \propto (0.4 \div 0.6) \times 10^{-4}$ cm]. With such dimensions, the diffusion of the main charge carriers in the base i-region can be neglected because the irradiation penetration depth $1/\alpha$ is higher than base thickness $d(1/\alpha \propto 10^4 \text{cm}, \alpha d < 1)$ (about absorption coefficient α see below, expression (20) and Fig. 2). For the drift approximation, it is also important that the length of the base region and the diffusion lengths of charge carriers in halide perovskites are of the same order of magnitude (0.4-2) μm[31,47,].Then it can be assumed that changes in the concentration of photocarriers along the depth of the i-th layer will be very weak and independent from the coordinate. With such an approximation, the diffusion currents will simply be neglected.

Hence from Eq.(4) follows:

$$J_{ph} \approx en\mu_n E + ep\mu_p E = e\Delta n\mu_n E + e\Delta p\mu_p E = e\Delta n\mu_p E(b+1), \quad ...(7)$$

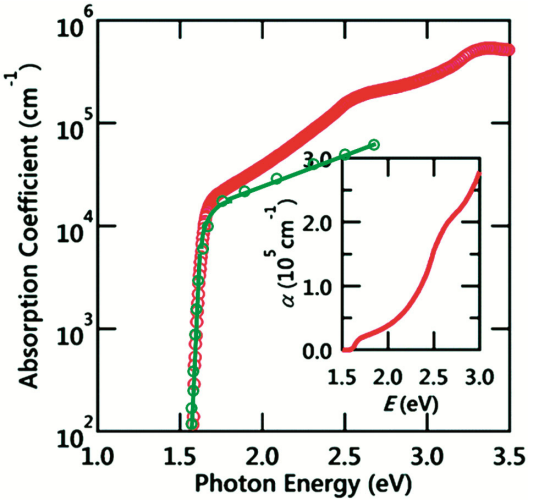

Fig. 2 — Spectral dependency of absorption coefficient. Red cycles data is adapted from[68], the green squares noted the data calculated from the Eq. (20).

where $b \equiv \mu_n/\mu_p$. From Eqs.(5) we have:

$$\mu_n\Delta n\frac{\partial E}{\partial x} = \frac{\Delta n}{\tau_n} - G, \qquad -\mu_p\Delta n\frac{\partial E}{\partial x} = \frac{\Delta n}{\tau_p} - G, \quad ...(8)$$

Sum of Eqs. (8) give

$$(\mu_n - \mu_p)\Delta n\frac{\partial E}{\partial x} = \Delta n\frac{\tau_n+\tau_p}{\tau_n\tau_p} - 2G,$$

from where we get

$$\frac{\partial E}{\partial x} = \frac{1}{\mu_p(b-1)\Delta n}\left(\Delta n\frac{\tau_n+\tau_p}{\tau_n\tau_p} - 2G\right). \quad ...(9)$$

The internal built-in electric field in the base region E arises due to the contact potential difference φ_c (see, Fig. 1). This field mainly falls on the high-resistance i -layer. Then, as a boundary condition for solving Eq. (9), one can use $E = 0$ at $x = 0$ and $E = E$ at $x = d$. Then solution of Eq. (9) gives

$$E = \frac{d}{\mu_p(b-1)\Delta n}\left\{\Delta n\frac{\tau_n+\tau_p}{\tau_n\tau_p} - \frac{2\eta(\lambda)\alpha(\lambda)F_0}{\alpha d}[1 - exp(-\alpha x)]\right\} \quad ...(10a)$$

On the other side from Eq. (6) we have

$$E = \frac{J_{ph}}{e\Delta n\mu_p(1+b)}. \quad ...(10b)$$

After equalizing the right parts of Eqs. (10a) and (10b), we obtain expression for photocurrent:

$$J_{ph} = \frac{ed(b+1)}{(b-1)}\left\{\Delta n\frac{\tau_n+\tau_p}{\tau_n\tau_p} - \frac{2\eta(\lambda)\alpha(\lambda)F_0}{\alpha d}[1 - exp(-\alpha x)]\right\}. \quad ...(11)$$

The photocurrent strongly depends on the concentration of photo carriers (*i.e.*, the incident radiation flux F_0) and the absorption coefficient. At the $V = 0$ we have $j_{sc}(\lambda) = j_{ph}(\lambda)$. The smaller the value of b, the higher the j_{sc}. Total current density will be:

$$J = J_s\left[exp\left(\frac{eV}{mkT}\right) - 1\right] - \frac{ed(b+1)}{(b-1)}\left\{\Delta n\frac{\tau_n+\tau_p}{\tau_n\tau_p} - \frac{2\eta(\lambda)\alpha(\lambda)F_0}{\alpha d}[1 - exp(-\alpha x)]\right\}. \quad (12)$$

For dark saturation current we have:

$$J_s = e\left(\frac{D_n n_p}{L_n} + \frac{D_p p_n}{L_p}\right) = kT\left(\frac{\mu_n n_p}{L_n} + \frac{\mu_p p_n}{L_p}\right). \quad ...(13)$$

Here n_p and p_n are concentrations of minority carriers, L_n and L_p are diffusion lengths of electrons and holes.

A-priory fill factor is determined as

$$FF = \frac{I_{mp}V_{mp}}{I_{sc}V_{oc}} = \frac{J_{mp}V_{mp}}{J_{sc}V_{oc}} \quad ...(14)$$

For determination of maximum power current J_{mp} and maximum power voltage V_{mp} the following is done. Power produced by the cell P is the product of the voltage and the current, i.e.

$$P = IV = AJV, . \quad ..(15)$$

Where A is the surface area of SC. Maximum power voltage V_{mp} occurs when $\frac{dP}{dV} = 0$, and is equal to

$$V_{mp} = V_{oc} - \frac{mkT}{e} ln\left(1 + \frac{eV_{mp}}{mkT}\right). \quad ...(16)$$

This is an implicit equation and has no simple solution. As it is shown in Ref. [48] the initial guess $V_{mp} = 0.9V_{oc}$ gives the exact solution in two iterations.

Maximum power current will be equal to

$$J_{mp} = J_s\left[exp\left(\frac{eV_{mp}}{mkT}\right) - 1\right] - \frac{ed(b+1)}{(b-1)}\left\{\Delta n\frac{\tau_n+\tau_p}{\tau_n\tau_p} - \frac{2\eta(\lambda)\alpha(\lambda)F_0}{\alpha d}[1 - exp(-\alpha x)]\right\}. \quad ...(17)$$

Then

$$FF = \frac{J_{mp}V_{mp}}{J_{sc}V_{oc}} \approx 0.9 \times \left\{\frac{J_s}{J_{sc}}\left[exp\left(\frac{eV_{mp}}{mkT}\right) - 1\right] - 1\right\}. \quad ...(18)$$

The power conversion efficiency (PCE) will be calculate by the following expression

$$\eta = \frac{J_{mp}V_{mp}}{P_m}, \quad ...(19)$$

where P_m is the input power density.

3 Numerical Simulation

Numerical modeling of solar cells with p-i-n structure was performed on $CH_3NH_3PbI_3$ using "Microsoft Excel spreadsheet software". There are different values for carrier mobility, lifetimes and diffusion constants in the literature for thin films. Some of them are presented in Table 1 (by prefix e and h are noted electron and hole).

Measurements for direct bandgap energy of $CH_3NH_3PbI_3$ give $E_g = 1.56$ eV[44,45]. According to the band structure theory for a direct bandgap semiconductors, absorption in the region close to the beginning of absorption $\propto (E_{ph} - E_g)^{1/2}$, where E_{ph} is the photon energy[40]. Then using measurement data from Ref. [67] (Fig. 3(a)) and from Ref. [68] (Fig. 3) we can find following approximate expression for absorption coefficient spectral dependency $\alpha(\lambda)$:

Table 1 — Mobility, lifetimes and diffusion constants of $CH_3NH_3PbI_3$.

μ (cm²/Vs)	e(5-10)[30]; e(24±6.8)[49]; h(1-5)[30] (0.3-6.7)[50]; (10-34)[51]; (0.4-71)[52]; (66±8)[47]
τ (μs)	14.7[47];6[53]; (21-54)[54]; 15[55]; 1.6[56]; 0.0053[57]; (82 ± 5)[50];(95 ± 8)[50];≥ 32[58]
D (cm²/s)	e(1.64)[47]; e(0.01-4)[53,59]; h(0.029)[50]; h(0.76)[38] (1.64±0.15)[47];(1.7±0.1)[57]; (0.01-0.2)[60]; (0.02-0.16)[15,61,62]; (0.05-1.77)[63-66]

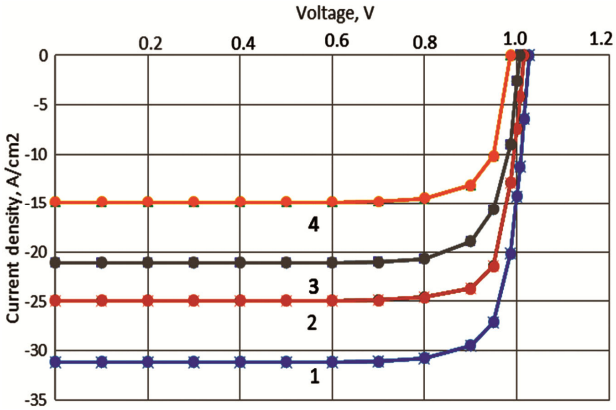

Fig. 3 — Current-voltage characteristics for p-i-n perovskite SC. Curves correspond following cases: 1 - $\lambda = 0.7$μm ($h\nu = 1.77$eV); 2 -$\lambda = 0.75$μm ($h\nu = 1.65$eV); 3 - $\lambda = 0.77$μm ($h\nu = 1.61$eV), 4 - $\lambda = 0.79$μm ($h\nu = 1.57$eV).

$$\alpha(h\nu) = 3.65 \times 10^4 \left(h\nu - E_g\right)^{1/2} \text{or } \alpha(\lambda) = 3.65 \times 10^4 \left(\frac{1.24}{\lambda} - E_g\right)^{1/2} \quad ...(20)$$

Here $\alpha(h\nu)$, $h\nu$ and λ given in cm^{-1}, eV and μm, correspondingly. Fig. 2 shows measurement data from Ref. [68] for the dependence $\alpha(h\nu)$ and the curve plotted according to Eq. (20). The coincidence is very good near the perovskite absorption edge of 1.5-2 eV.

The energy flux of sunlight reaching the surface of the earth is $1.388\times10^3 \text{W/m}^2$. For $CH_3NH_3PbI_3$ E_g =1.56 eV and photon flux is equal to

$$F_0 = \frac{1.388\times10^3 \text{Wm}^{-2}}{1.56 \text{ eV}} = 5.5533 \times 10^{17} \text{cm}^{-2}\text{s}^{-1}.$$

Taking into account some losses of solar energy before entering the base region of the structure, $F_0 \approx 10^{17}\text{cm}^{-2}\text{s}^{-1}$ is used in further calculations. On the base of data from Table 1 for further simulation we use following parameters for i-type $CH_3NH_3PbI_3$ $E_g = 1.56$ eV, electron affinity 3.9 eV,$d = 4 \times 10^{-5}$ cm: $\mu_n \approx 5$ cm^2/Vs and $\mu_p \approx 1$ cm^2/Vs $(b = 5)$, $\eta(\lambda) \approx 1$, $F_0 \approx 10^{17}\text{cm}^{-2}\text{s}^{-1}$, $\Delta n \approx 10^{17}\text{cm}^{-3}$,$D_n \approx 1.64$ cm^2/s, $D_p \approx 0{,}029$ cm^2/s, $\tau_n \approx 1.25 \times 10^{-3}\text{s}$, $\tau_p \approx 1.25 \times 10^{-4}s$, $m = 2$, $n_p \approx p_n \approx 10^7\text{cm}^{-3}$, $P_m \approx 1\,\text{kW/m}^2 = 100$ mW/cm^2.

Note that perovskites are known to have low trap densities[69]. In the process of modeling the parameters of p-i-n SCs, the influence of lattice defects, interfaces and related effects (changes in lifetime, mobility, *etc.*) is not taken into account. It is clear that in real elements they will influence the generation and recombination of current carriers. The idealized model takes into account only generation-recombination processes, in which only the material's own atoms participate.

Fig. 3 shows I-V characteristics for four cases of wavelength. Fig. 4 shows spectral dependency of J_{sc} and V_{oc}. In the Table 2 the data of V_{oc}, V_{mp}, J_{sc}, J_{mp} and FF (calculated according Eq. (18)) are presented for the four cases of wavelength.

4 Results and Conclusion

The short circuit current strongly depends on the carrier mobility ratio ($b = \mu_n/\mu_p$), but not on the mobility of electrons or holes themselves. The smaller the value of b, the greater the J_{sc}. This can be explained as follows: the smaller b, the closer the values of the electron and hole mobilities. This means that charge carriers will not linger and collect in the base region, and the rate of carrier recombination will decrease. As a result, electrical losses will decrease and the J_{sc} will increase.

Closer to the edge of intrinsic absorption, J_{sc} and V_{oc} depend linearly on the wavelength of the incident radiation. Calculations show the potential use of perovskites in the design of tandem SCs. This material provides good absorption of solar photons with energy >1.56 eV. In combination with crystalline Si, perovskite can broaden the absorption spectrusm of radiation, thereby increasing the PCE of solar cells. It is clear that both J_{sc} and V_{oc} are limited by the saturation current of the diode structure. They depend on the parameters of the source material. By adjusting them, it will be possible to choose the optimal parameters of the SC.

Data on J_{sc} and V_{oc} obtained by us (~15÷31 mA/cm^2, ~0.99÷1.03 V), are in good agreement with the results of previous numerical and experimental data for $CH_3NH_3PbI_3$ with similar dimensions. The values for FF and the PCE obtained

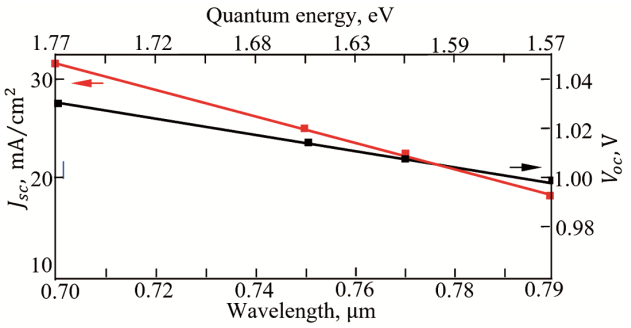

Fig. 4 — Spectral dependency of short-circuit current and open-circuit voltage.

Table 2 — Main parameters $CH_3NH_3PbI_3$ based solar cell.

λ(μm)	0.70	0.75	0.77	0.79
V_{oc} (V)	1.03	1.02	1.01	0.99
V_{mp} (V)	0.92	0.91	0.906	0.89
J_{sc} (mA/cm^2)	31.17	24.95	21.70	18.3
J_{mp} (mA/cm^2)	29.40	23.32	19.84	16.71
FF (%)	84.8	84.1	82.3	82.1
η(%)	27.20	21.30	17.98	14.85

by us are quite good and corresponds with data of literature. Data for J_{sc}, V_{oc}, V_{mp}, J_{mp}, FF and η for four incident irradiation wavelengths are presented in Table 2.

Funding: The investigation is carried out with the financial support of the Science Committee of the Republic of Armenia within the framework of Scientific Project No. 21AG-2B011.

Competing Interests: The author declare no competing financial interest.

Data Availability

The data that support the findings of this study are available within the article.

Consent for Publication

I agree for publication of my article.

Conflict of Interest

There is no conflict of interest.

References

1 Uddin A, *Comprehensive Guide on Organic and Inorganic Solar Cells*, Elsevier, (2022) 25.
2 Dipta S S & Uddin A, *Reference Module in Earth Systems and Environmental Sciences*, Elsevier, (2022).
3 Tanveer K A M M, Khan M K R, Liton M N H, Kamruzzaman M, Hossain M S & Chen S, *AIP Advances*, 12 (2022) 065126.
4 Syahra N C, Iwantono, Rinia A S, Nurrahmawati P, Nafisah S, Morsin M & Syahputra R F, *Indian J Pure Appl Phys*, 61 (2023) 90.
5 Sarkar P, Mayengbam R, Tripathy S K & Baishnab K L, *Indian J Pure Appl Phys*, 57 (2019) 891.
6 Liu M, Johnston M B & Snaith H J, *Nature*, 501 (2013) 395.
7 Jeon N J, Noh J H, Kim Y C, Yang W S, Ryu S & Seok S I, *Nat Mater*, 13 (2014) 897.
8 Bai S, Wu Z, *et al*., *Nano Res*, 7 (2014) 1749.
9 Hernández-Granados A, Corpus-Mendoza A N, Moreno-Romero P M, Rodríguez-Castañeda C A, Pascoe-Sussoni J E, Castelo-González O A, Menchaca-Campos E C, Escorcia-García J & Hu H, *Opt Mater*, 88 (2019) 695.
10 Tuchinda W, Amratisha K, *et al*., *Solar Energy*, 244 (2022) 65.
11 Park J Y, Lee Y H, Kim H & Dou L, *J Appl Phys*, 134 (2023) 060901.
12 Mei A, Li X, *et al*. *Science*, 345 (2014) 295.
13 Green M A, Dunlop E D, Hohl-Ebinger J, Yoshita M, Kopidakis N, Bothe K, Hinken D, Rauer M & Hao X, *Prog Photovolt Res Appl*, 30 (2022) 687.
14 Lang F, Jošt M, Frohna K, *et al*., *Joule*, 4 (2020) 1054.
15 Xing G, Mathews N, Lim S S, Yantara N, Liu X, Sabba D, Grätzel M, Mhaisalkar S & Sum T C, *Nat Mater*, 13 (2014) 476.
16 Zhang Q, Shang Q, Su R, Do T T H & Xiong Q, *Nano Lett*, 21 (2021) 1903.
17 Tan Z K, Moghaddam R S, Lai M L, *et al*., *Nat Nanotechnol*, 9 (2014) 687.
18 Liu X K, Xu W, Bai S, Jin Y, Wang J, Friend R H & Gao F, *Nat Mater*, 20 (2021) 10.
19 Li G, Wang Y, Huang L & Sun W, *ACS Appl Electron Mater*, 4 (2022) 1485.
20 Dong R, Fang Y, Chae J, Dai J, Xiao Z, Dong Q, Yuan Y, Centrone A, Zeng X C & Huang J, *Adv Mater*, 27 (2015) 1912.
21 Dou L, Yang Y, You J, Hong Z, Chang W-H, Li G & Yang Y, *Nat Commun*, 5 (2014) 5404.
22 Green M A, Dunlop E D, Yoshita M, Kopidakis N, Bothe K, Siefer G & Hao X, *Prog Photovoltaics*, 31 (2023) 651.
23 Al-Ashouri A, Köhnen E, Li B, *et al.*, *Science*, 370 (2020) 1300.
24 Yoo J J, Seo G, *et al*., *Nature*, 590 (2021) 587.
25 Jeong J, Kim M, *et al*., *Nature*, 592 (2021) 381.
26 YingZ, Yang Z, *et al*., *Joule*, 6 (2022) 2644.
27 Yin W-J, Yang Ji-H, Kang J & Yan S-H, *J Mater Chem*, A3 (2015) 8926.
28 Tooghi A, Fathi D & Eskandari M. *Sci Rep*, 10 (2020)18699.
29 Hossain M F, Faisal M & Okada H, *2nd Int Conf on Electrical, Computer & Telecom Engineering (ICECTE)*, Rajshahi, Bangladesh, (2016) 1.
30 Motta C, El-Mellouhi F & Sanvito S, *Sci Rep*, 5 (2015) 12746.
31 Akel S, Kulkarni A, Rau U & Kirchartz T, *Prx Energy*, 2 (2023) 013004.
32 Radhakrishna K, Manjunath S B, Devadiga D, Chetri R & Nagaraja A T, *ACS Appl Energy Mater*, 6 (2023) 3635.
33 Rakstys K, Paek S, Drevilkauskaite A, Kanda H, Daskeviciute S, Shibayama N, Daskeviciene M, Gruodis A, Kamarauskas E, Jankauskas V, Getautis V & Nazeeruddin M K, *ACS Appl Mater Interf*, 12 (2020) 19710.
34 Meng X, Ho C H Y, Xiao S, Bai Y, Zhang T, Hu C, Lin H, Yang Y, So S K & Yang S, *Nano Energy*, 52 (2018) 300.
35 Kong J, Wang H, *et al. ACS Appl Energy Mater*, 3 (2020) 7231.
36 Peng J, Kremer F, Walter D, *et al*., *Nature*, 601 (2022) 573.
37 Li C, Zhang Y, Zhang X, Zhang P, Yang X & Chen H, *Adv Funct Mater*, 33 (2023) 2214774.
38 Chen L-C, Chen J-C, Chen C-C & Wu C-G, *Nanoscale Res Lett*, 1 (2015) 1020.
39 Dharmadasa I M, Rahaq Y & Alam A E, *J Mater Sci: Mater Electron*, 30 (2019) 12851.
40 Moss T S, Barrell G J & Ellis B, *Semiconductor Opto-Electronics*, Bullerworth & Co. LTD, (1973).
41 Kumar A, Singh S & Al-Bahrani M, *Surfaces Interfaces*, 34 (2022) 102341.
42 Ghosekar I C & Patil G C, *Semicond Sci Technol*, 36 (2021) 045005.
43 Gasparyan F V & Ayvazyan G Y, *J Contemp Phys,* 53 (2022) 160.
44 Ayvazyan G, Vaseashta A, Gasparyan F & Khudaverdyan S, *J Mater Sci.: Mater Electron*, 33 (2022) 17001.
45 Ayvazyan G, Gasparyan F & Gasparian V, *Opt Mater*, 140 (2023) 113879.
46 Park S, *Irradiation effect in triple junction solar cells for spatial applications*, (2019).
47 Dong Q, Fang Y, Shao Y, Mulligan P, Qiu J, Cao L & Huang J, *Science*, 347 (2015) 967.

48 https://www.pveducation.org/pvcdrom/voltage-at-the-maximum-power-point-vmp.
49 Lim J, Kober-Czerny M, Lin Y-H, Ball J M, Sakai N, Duijnstee E A, Hong M J, Labram J G, Wenger B & Snaith H J, *Nat Commun*, 13 (2022) 4201.
50 Wehrenfennig C, Liu M, Snaith H J, Johnston M B & HerzL M, *J Phys Chem Lett*, 5 (2014) 1300.
51 Herz L M, *ACS Energy Lett*, 2 (2017)1539.
52 Pasanen H P, Vivo P, Canil L, Hempel H, Unold T, Abate A & Tkachenko N V, *J Phys Chem Lett*, 11 (2020) 445.
53 Yang X, Fu Y, *et al., Adv Mater*, 32 (2020) 2002585.
54 Chouhan A S, Jasti N P, Hadke S, Raghavan S & Avasthi S, *Curr Appl Phys*, 17 (2017) 1335.
55 Bi Y, Hutter E M, Fang Y, Dong Q, Huang J & Savenije T J, *J Phys Chem Lett*, 7 (2016) 923.
56 Bou A, Bboliņš H A, Ashoka A, Cruanyes H, Guerrero A, Deschler F & Bisquert J, *ACS Energy Lett*, 6 (2021) 2248.
57 Webber D, Clegg C, Mason A W, March S A, HillI G & Hall K C, *Appl Phys Lett,* 111 (2017) 121905.
58 Wehrenfennig A, Liu M, Snaith H J, Johnston M B & Herz L M, *Energy Environ Sci*, 7 (2014) 2269.
59 Xia C Q, Peng J, *et al*. *J Phys Chem Lett*, 12 (2021) 3607.
60 Guo Z, Zhou N, Williams O F, Hu J, You W & Moran A M, *J Phys Chem C*, 122 (2018) 10650.
61 Savenije T J, Ponseca C S, *et al.*, *J Phys Chem Lett*, 5 (2014) 2189.
62 Xing G, Mathews N, Sun S, Lim S S, LamY M, Gratzel M, Mhaisalkar S & Sum T C, *Science*, 342 (2013).
63 Guo Z, Wan Y, Yang M, Snaider J, Zhu K & Huang L*, Science*, 356 (22017) 59.
64 Guo Z, Manser J S, Wan Y, Kamat P V & Huang L, *Nat Commun*, 6 (2015) 7471.
65 Tian W, Zhao C, Leng J, Cui R & Jin S, *J Am Chem Soc*, 137 (2015) 12458.
66 Hill A H, Smyser K E, Kennedy C L, Massaro E S & Grumstrup E M*, J Phys Chem Lett*, 8 (2017) 948.
67 Leguy A M A, Azarhoosh P, *et al*., *Nanoscale*, 8 (2016) 6317.
68 Kanemitsu Y, *J Mater Chem C*, 5 (2017) 3427.
69 Bhandari K P & Ellingson R J, *In book: A Comprehensive Guide to Solar Energy Systems*, Letcher T M, Fthenakis V M, Eds.; Academic Press, (2018) 233.